SAND2018-9193C

Adventures in Vibrational Spectroscopy at Clay Edges: Can Experiments and Molecular Modeling Agree?

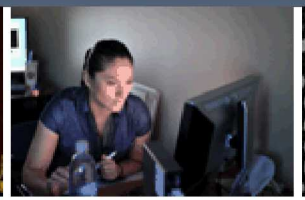

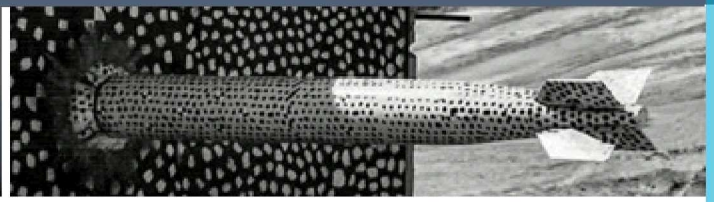

PRESENTED BY

Jacob A. Harvey,[1] Cliff T. Johnston,[2] Jeffery A. Greathouse[1]

[1]Geochemistry Department, Sandia National Laboratories, Albuquerque, New Mexico 87125, United States

[2]. Crop, Soil and Environmental Sciences, Purdue University, West Lafayette, Indiana 47907, United States

Sandia National Laboratories is a multimission laboratory managed and operated by National Technology & Engineering Solutions of Sandia, LLC, a wholly owned subsidiary of Honeywell International Inc., for the U.S. Department of Energy's National Nuclear Security Administration under contract DE-NA0003525.

Acknowledgements

This work was supported by the U.S. Department of Energy, Office of Science, Office of Basic Energy Sciences, Chemical Sciences, Geosciences, and Biosciences Division and Laboratory Directed Research and Development Program at Sandia National Laboratories. Sandia National Laboratories is a multimission laboratory managed and operated by National Technology and Engineering Solutions of Sandia, LLC., a wholly owned subsidiary of Honeywell International, Inc., for the U.S. Department of Energy's National Nuclear Security Administration under contract DE-NA-0003525.

Molecular Simulation of Phyllosilicates

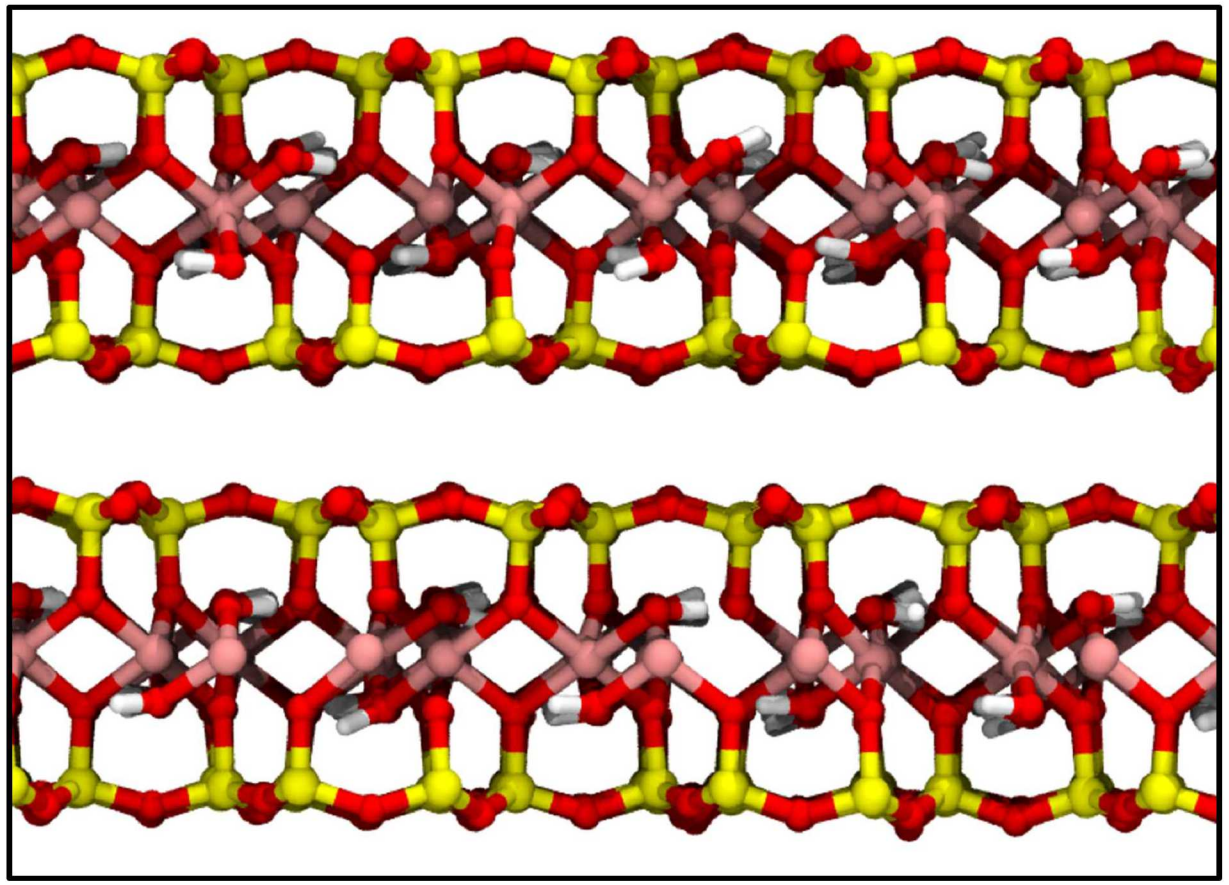

- Phyllosilicates exist as TOT stacked sheets
- Stacking disorder complicates structural analysis
- Complex chemistry with multicomponent systems, cation disorder, and vacancies
- Substitutions create a charge imbalance which is satisfied with cations in the interlamellar layer
- Swelling occurs which requires fully flexible force fields

ClayFF Force Field Past Successes

Swelling of Clays

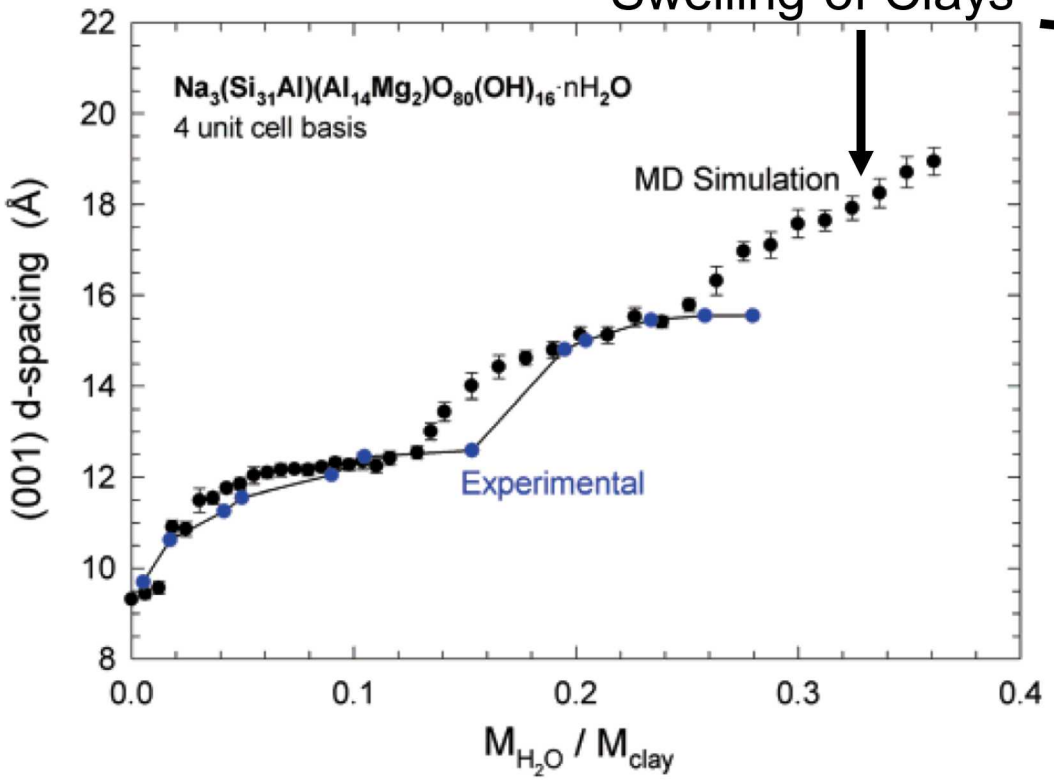

$$E_{total} = E_{Coul} + E_{VDW} + E_{BondO-H}$$

$$E_{total} = \frac{q_i q_j}{4\pi\epsilon_\circ r} + 4\epsilon_{ij}\left[\left(\frac{\sigma_{ij}}{r}\right)^{12} - \left(\frac{\sigma_{ij}}{r}\right)^{6}\right] + D_\circ\left[1 - e^{-\alpha(r-r_\circ)}\right]^2$$

		0W		1W		2W	
		this work	exp	this work	exp	this work	exp
Na^+	mont	9.35	9.6–9.8[21,58–61]	12.17	12.3–12.6[21,55,58]	14.91	14.9–15.6[21,55,58,59,61]
	beid	9.42	9.6–9.8[a,b,c]	12.26	12.4–12.5[a,b,c],		15.2–15.4[a]
Cs^+	mont	10.53	10.7–11.2[21,58–61]	12.28	11.9–12.6[58–60]		
	beid	10.93		12.27			
Ca^{2+}	mont	9.35		11.95		14.61	15.4–16.0[21,62,63]
	beid	9.32		11.94	11.78[d]		15.50[b]
Mg^{2+}	mont	9.30				13.61	13.9–14.9[64,65]
	beid	9.30		12.17		13.51	

Binding of organics at clay surfaces

		binding energy (kcal·mol^{-1})	
surface	complex	DFT	classical
gas phase	Ca^{2+}–DHNA$^-$	−345.4	−365.7
	Na^+–DHNA$^-$	−164.5	−150.1
	Na^+–toluene	−36.1	−13.1
pyrophyllite	Na^+	−101.5	−69.1
	Ca^{2+}	−350.1	−238.2
	DHNA	−16.3	−9.7
	Ca^{2+}–DHNA$^-$	−465.6	−402.8
kaolinite	Na^+	−89.4	−74.2
	DHNA	11.6	−12.4
	Na^+–DHNA$^-$	−188.8	−200.8
	toluene	−13.2	−13.4
	Na^+–toluene	−126.7	−91.0
	hexane	−11.2	−8.6
	cyclohexane	−10.7	−7.6

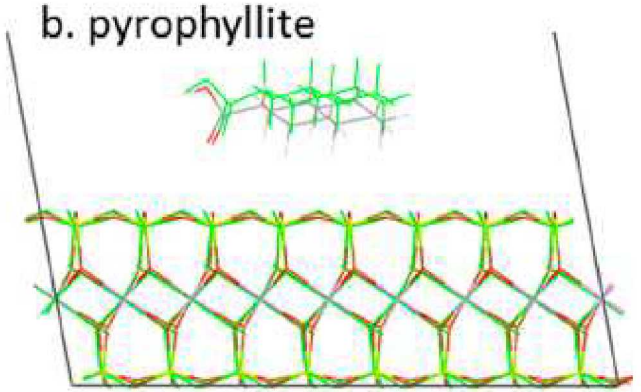

- Clayff has successfully modeled interactions, structures, and dynamics in bulk clays at the basal surface
- **But what about clay edges?**

Cygan, R.T. et al.; *J. Phys. Chem. B* **2004**, 108, 1255-1266
Teich-McGoldrick, S.L. et. al; *J. Phys. Chem. C* **2015**, 119, 20880
Greathouse, J.A. et. al; *J. Phys. Chem. C* **2017**, 121, 2273-22786

Parameters

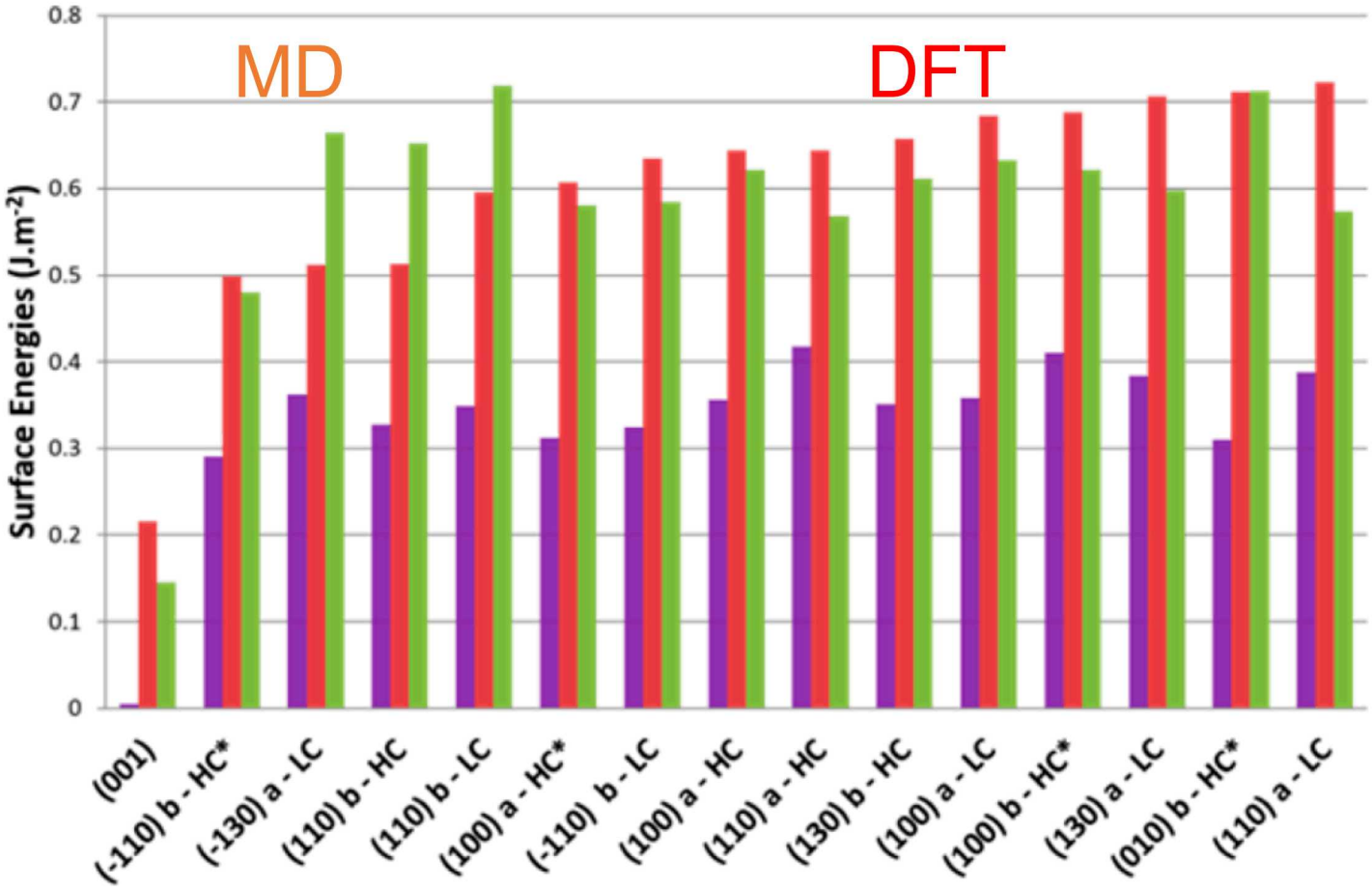

Bond	AC	Churakov (2006)
Si^1–OH	1.580	1.654
Si^2–OH	1.580	1.665
Al–OH_2	2.130	2.068
Al_2–OH	1.985	1.926
O–H	0.873	0.979[b]
(Si^1O)–Al	1.850	1.810
Si^1–(OAl)	1.580	1.665

- Surface energies of non-bonded ClayFF vs DFT have errors of up to 30%
- Edge Si-OH bond lengths are underestimated, Al-OH bond lengths are overestimated

Martins, D.M.S. et al.; *J. Phys. Chem. C* **2014**, 118, 27308-27317
Newton, A.G; Sposito, G.; Clays Clay Miner. **2015**, 63, 277-289

Parameters

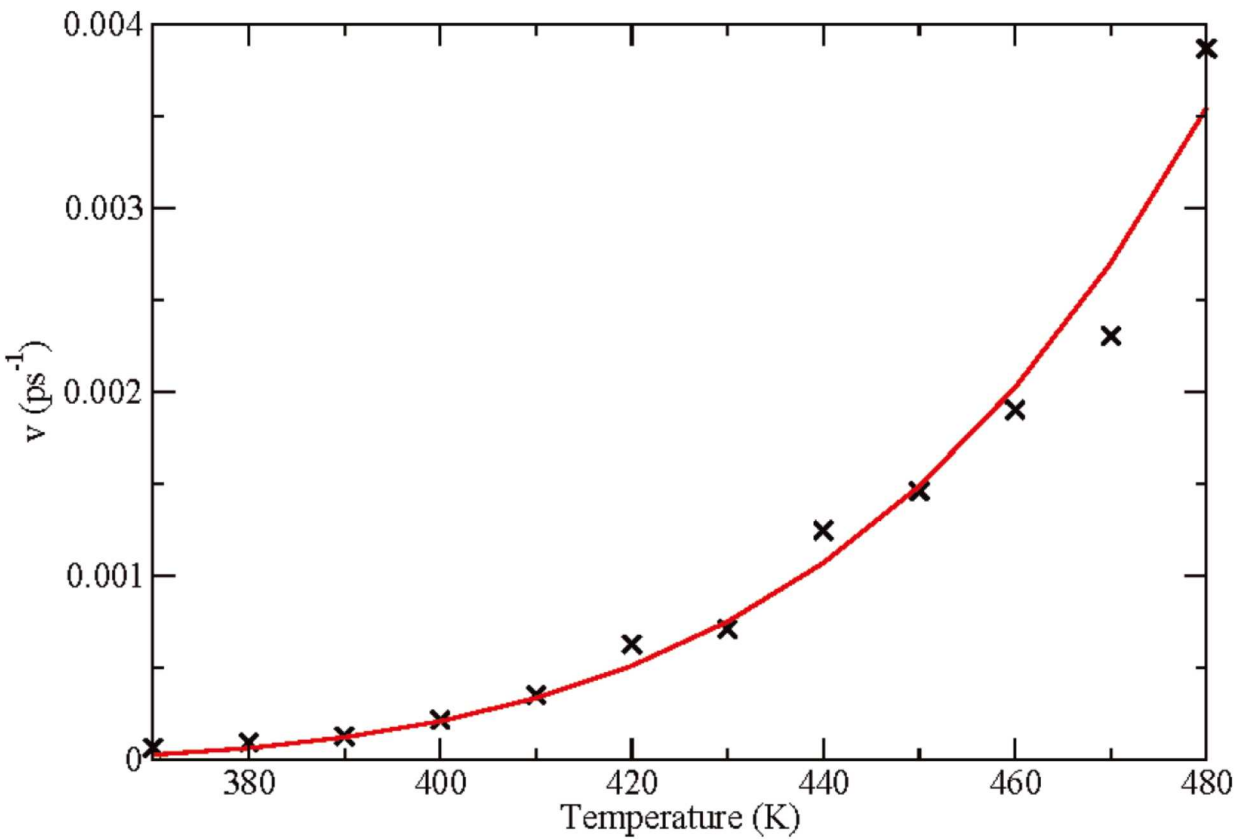

Reparametrization of atom charges

	original ClayFF	modified ClayFF	DFT
	Charges (e)		
H	0.425	0.464	
O	−0.871	−1.113	
Al	1.575	2.018	
Mg	1.050	1.438	
	k (kJ·mol^{-1}·rad^{-2})		
Mg−O−H	250	53	
	Surface Energy (kJ·mol^{-1}·Å^{-2})		
[001]	3.81	3.84	2.40
[1$\bar{1}$0]	1.56	3.77	4.24
[100]	3.38	6.26	6.35

- Surfaces in ClayFF are unstable and often “melt” at significantly lower than expected temperatures

Yu, K; Schmidt, J.R.; *J. Phys. Chem. C* **2014**, 115, 1887-1898

Parameters

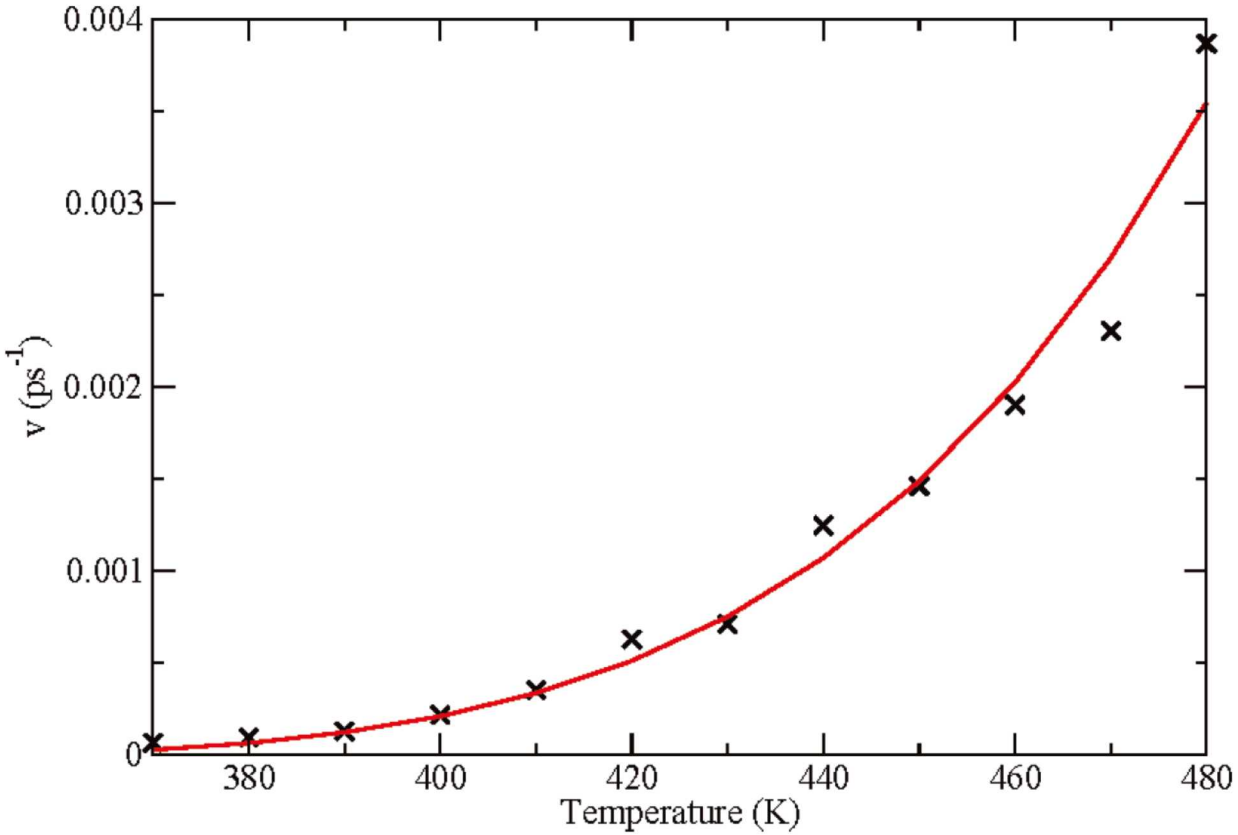

Reparametrization of atom charges

	original ClayFF	modified ClayFF	DFT
	Charges (e)		
H	0.425	0.464	
O	−0.871	−1.113	
Al	1.575	2.018	
Mg	1.050	1.438	
	k (kJ·mol^{-1}·rad^{-2})		
Mg−O−H	250	53	
	Surface Energy (kJ·mol^{-1}·Å^{-2})		
[001]	3.81	3.84	2.40
[1$\bar{1}$0]	1.56	3.77	4.24
[100]	3.38	6.26	6.35

- Surfaces in ClayFF are unstable and often “melt” at significantly lower than expected temperatures
- **Can we modify the ClayFF force field in way that is easy and consistent with previous results?**

Yu, K; Schmidt, J.R.; *J. Phys. Chem. C* **2014**, 115, 1887-1898

Effect of Angle Bending Parameters on Clay Structure

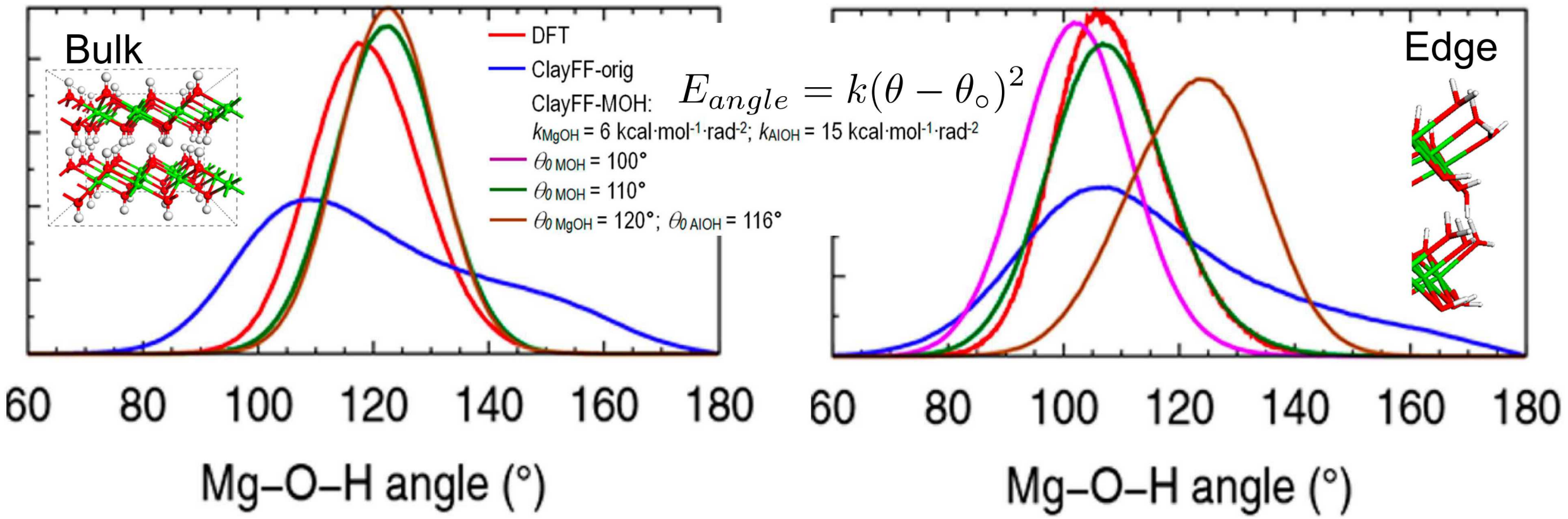

- Angle distributions from classical simulations with an angle bending term more closely match results from DFT simulations

Pouvreau, M. et. al; *J. Phys. Chem. C* **2017**, 121, 14757-14771

Effect of Angle Bending Parameters on Clay Structure

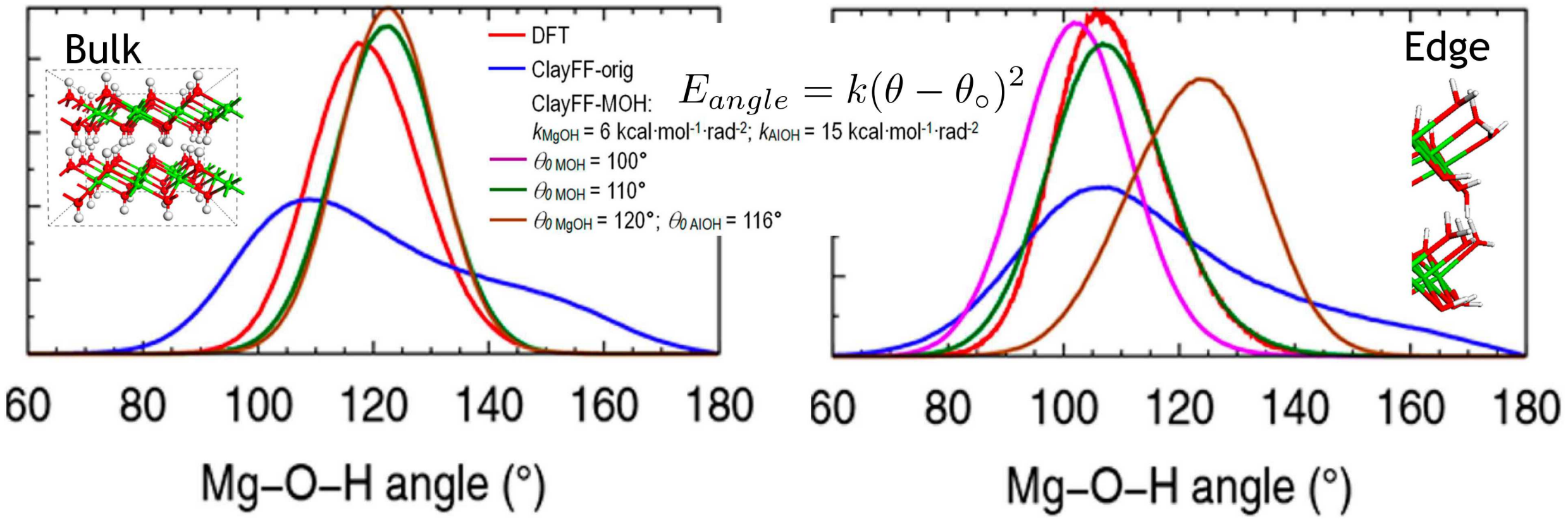

- Angle distributions from classical simulations with an angle bending term more closely match results from DFT simulations
- **Is this improved structure observable via infrared spectroscopy?**

Pouvreau, M. et. al; *J. Phys. Chem. C* **2017**, 121, 14757-14771

Pyrophyllite Model for Density Functional Theory Calculations

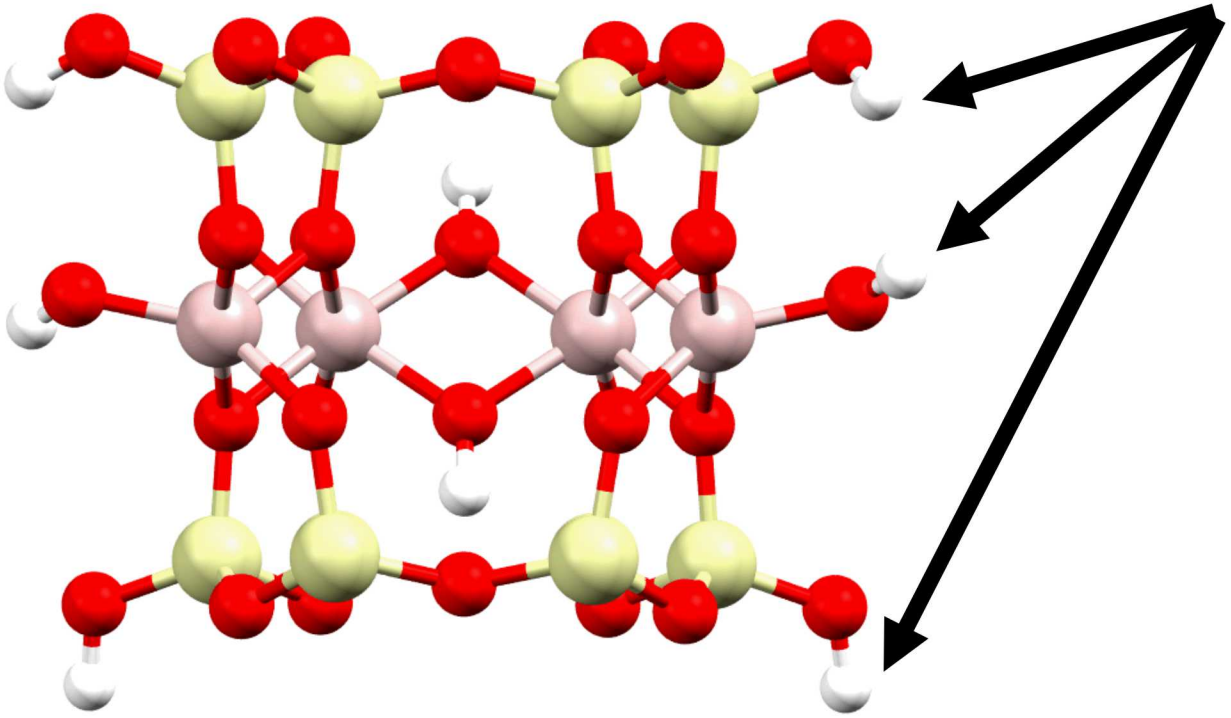

OD spectra replaces edge H's with D's

- Vibrational spectrum calculated on periodic structures using DFPT

$$I(\omega) = \sum_{\alpha=1}^{3} \left| \sum_{s=1}^{M} \sum_{\beta=1}^{3} Z^{*}_{\alpha\beta}(s) e_{\beta}(s) \right|^{2}$$

Cartesian polarizations

Vibrational eigenvector

Born effective charge of s^{th} atom

- 1x1x1 unit cell, (010) and (110) faces of pyrophyllite, 1 edge cut on each face
- VASP optimized/vibrational frequencies (PAW method, PBESol functional, DFT-D3 VDW corrections)
- Deuterate edges to compare to ATR-FTIR experiments where deuteration will only occur at edges
- Deuterated spectra are calculated from the protonated optimized structure

Phys. Rev. B **1991**, 43, 7231-7242; *J. Chem. Phys.* **1994**, 100, 8537-8539
Rev. Mod. Phys. **2001**, 73, 515-562; *J. Phys. Condens. Matt.* **2010**, 22, 265006

Pyrophyllite Edges

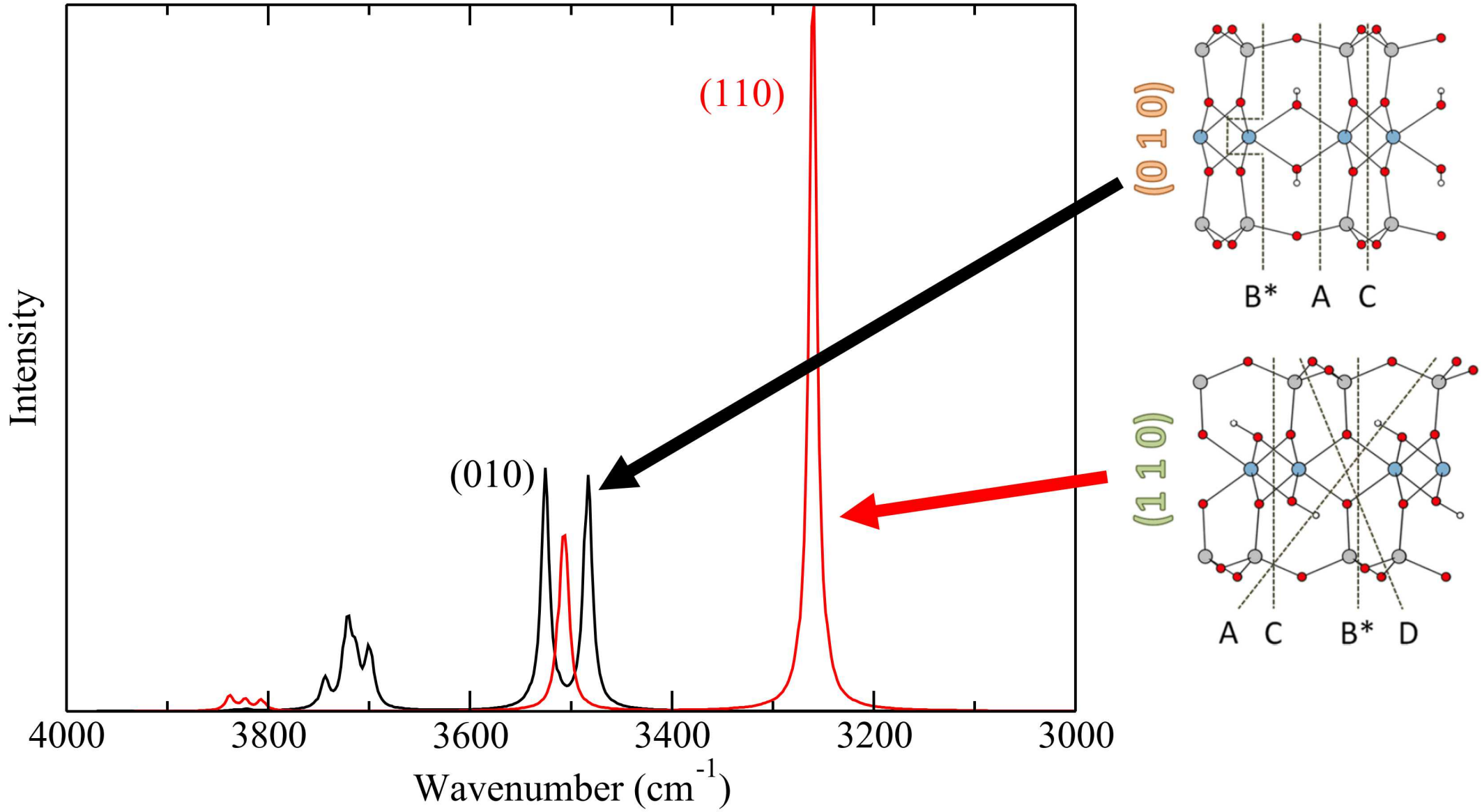

Hydrogen Bonding Features Observed in IR Spectra

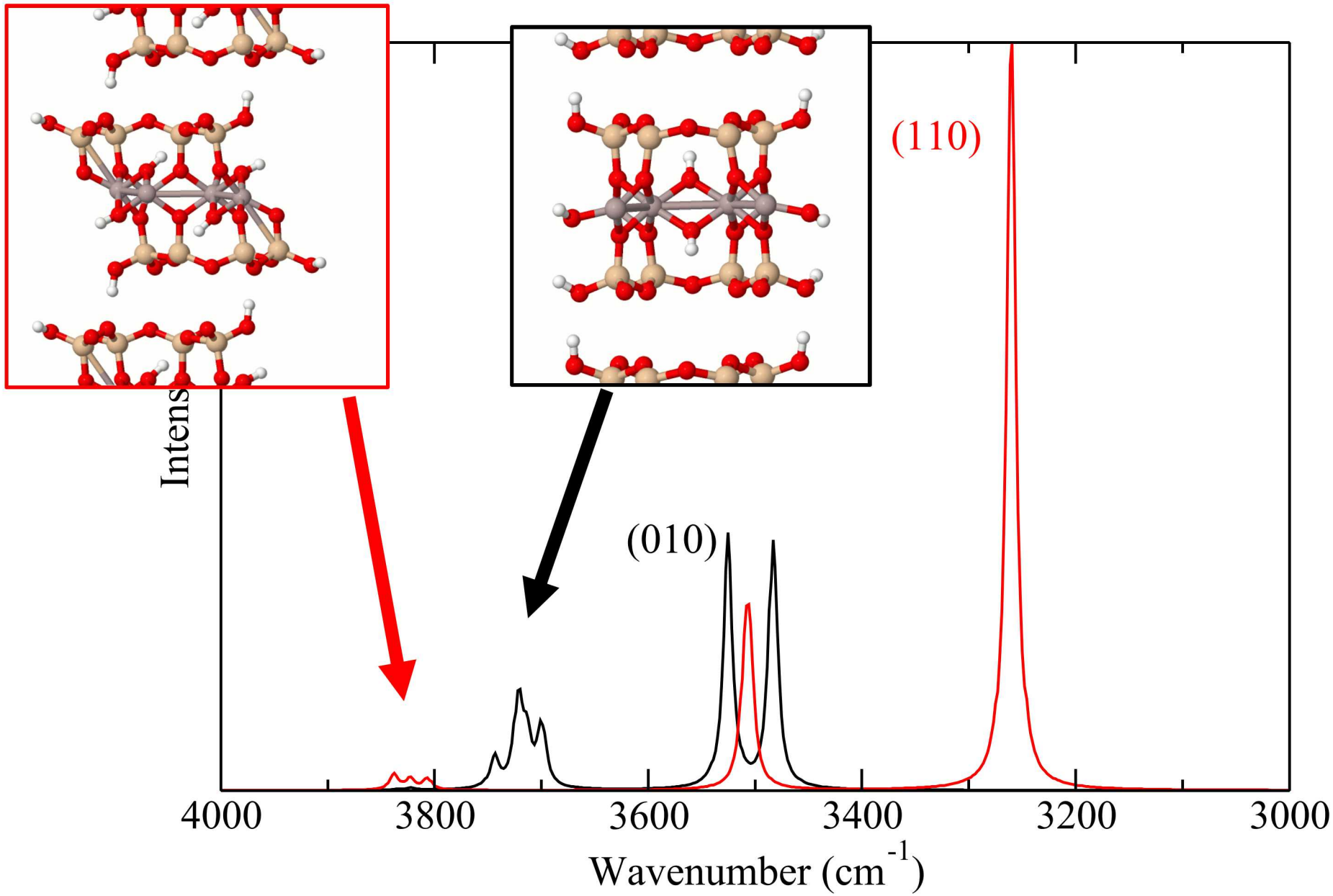

Hydrogen Bonding Features Observed in IR Spectra

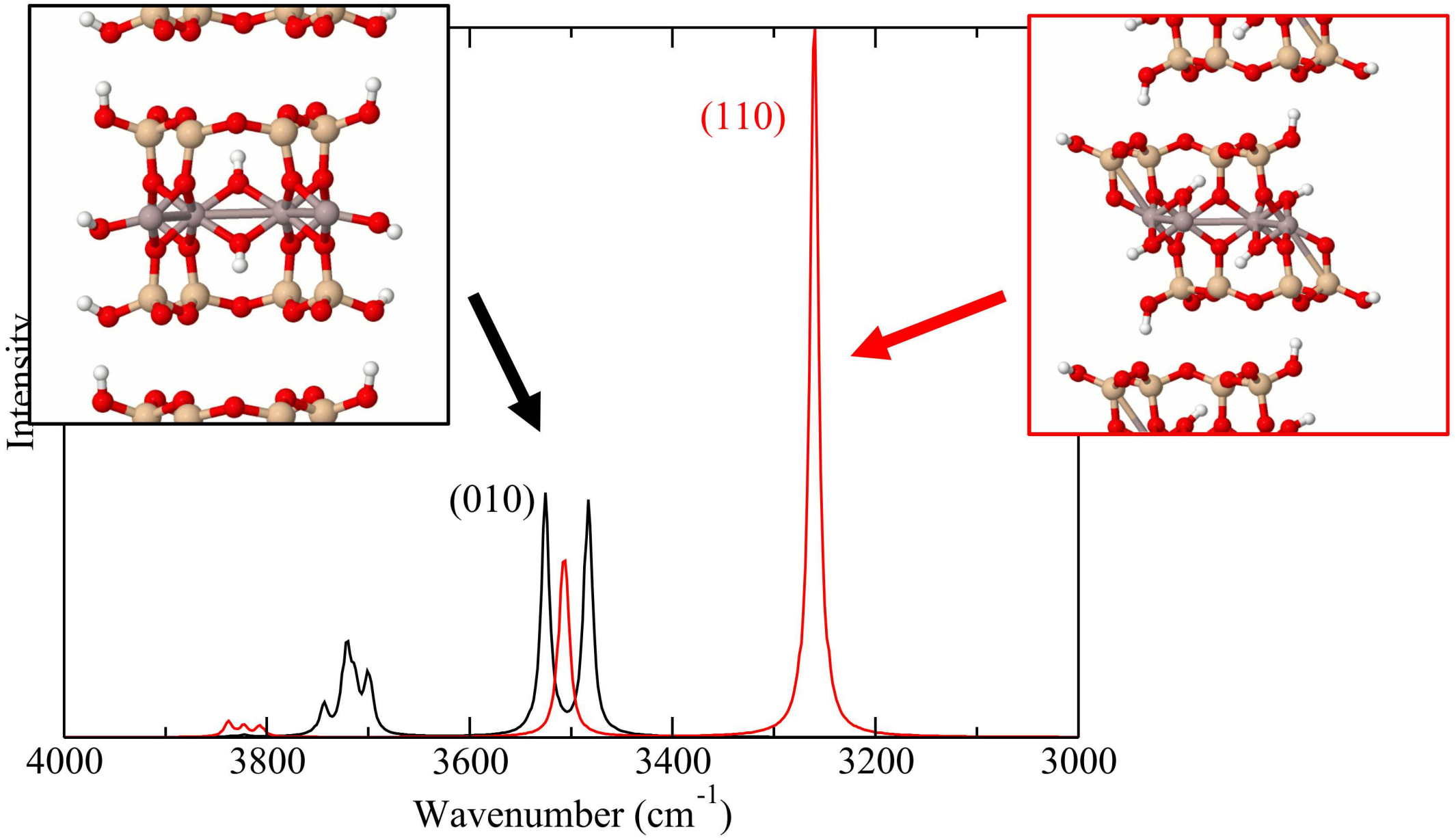

The Effect of Deuteration on IR Spectrum

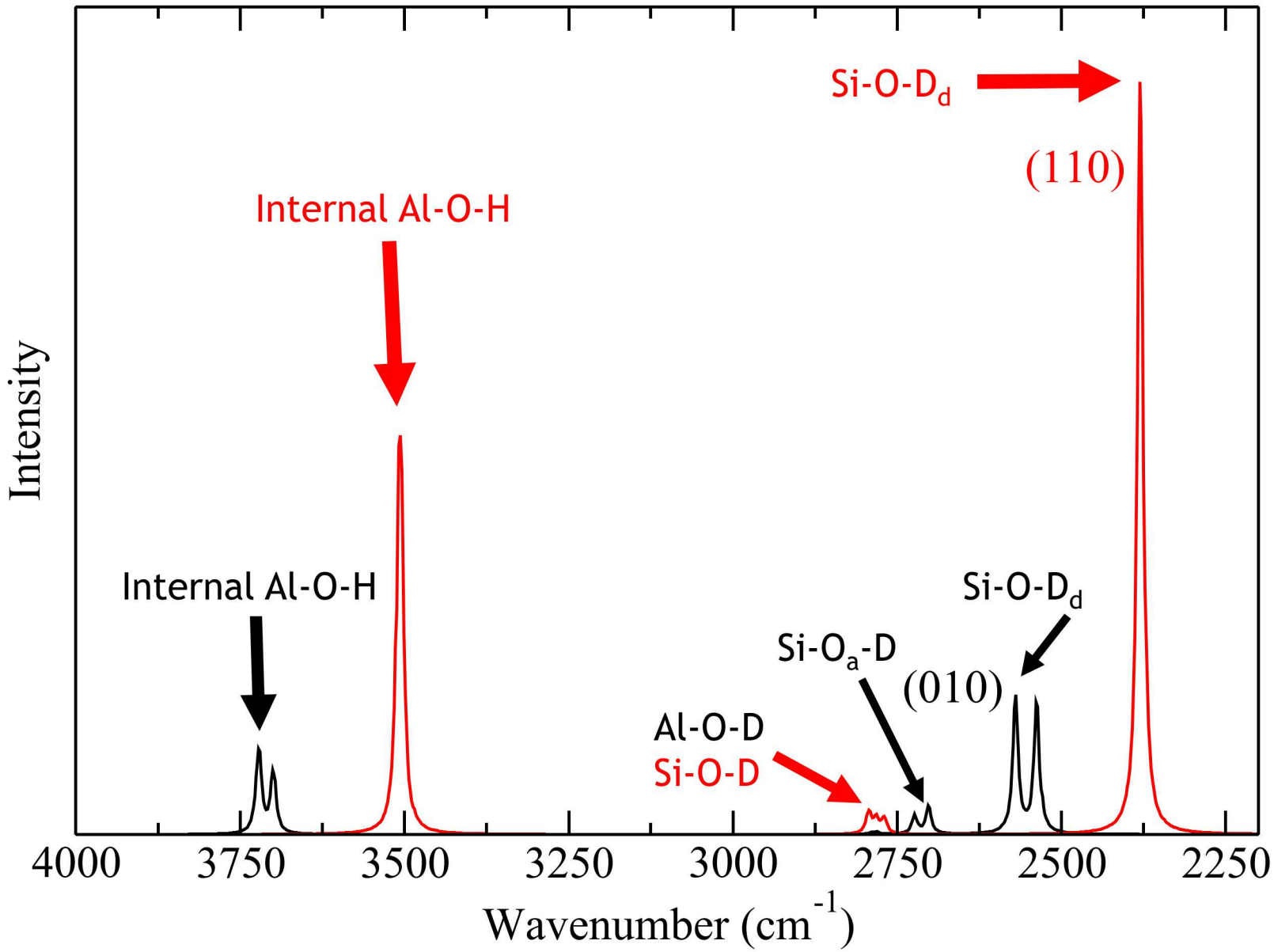

Molecular Dynamics Simulations of Pyrophyllite

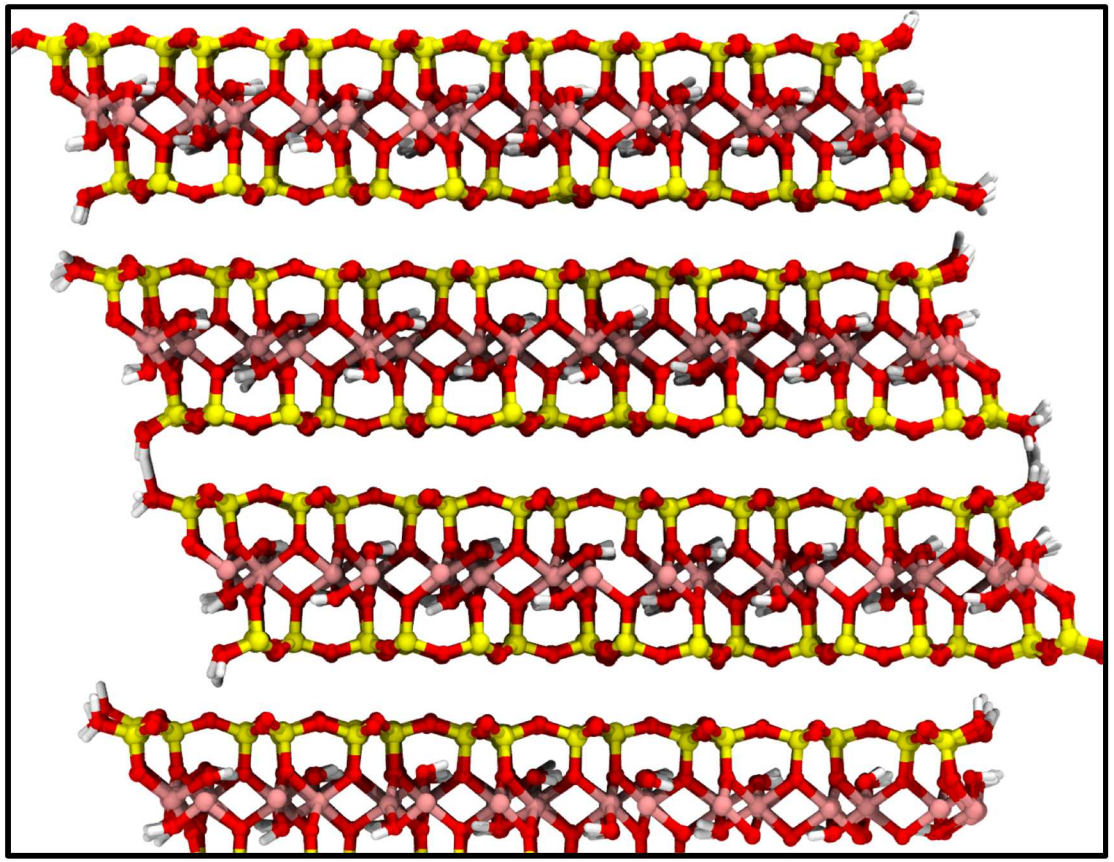

- 6x4x4 box created from optimized unit cells (3984 atoms)
- ClayFF force field with Al-O-H and Si-O-H angle bending parameters:

$$E_{angle} = k(\theta - \theta_\circ)^2$$

$$k = 15\ kcal/mol$$

$$\theta_\circ Si - O - H = 100^\circ$$

$$\theta_\circ Al - O - H = 110^\circ$$

- H/D atoms have different masses but same force field parameters
- NVT ensemble controlled by Nose-Hoover thermostat
- 10 ns equilibration time
- 5 ns of production run time, vibrational analysis over 1 ns
- Infrared Spectrum:

$$I(\omega) = \frac{1}{2\pi}\int_{-\infty}^{\infty} dt e^{-i\omega t}\langle \vec{M}(t)\cdot\vec{M}(0)\rangle \longrightarrow I(\omega) = \frac{1}{2\pi\omega^2}\int_{-\infty}^{\infty} dt e^{-i\omega t}\langle \frac{d\vec{M}(t)}{dt}\cdot\frac{d\vec{M}(0)}{dt}\rangle$$

$$\vec{M}(t) = \sum_{i}^{n_{atoms}} q_i\vec{r}_i(t) \qquad \frac{d\vec{M}(t)}{dt} = \sum_{i}^{n_{atoms}} q_i\vec{v}_i(t)$$

Al-O-H: Pouvreau, M. et. al; *J. Phys. Chem. C* **2017**, 121, 14757-14771
Si-O-H: Pouvreau, M. et. al **2017,** *in prep*.

from Correlation Functions

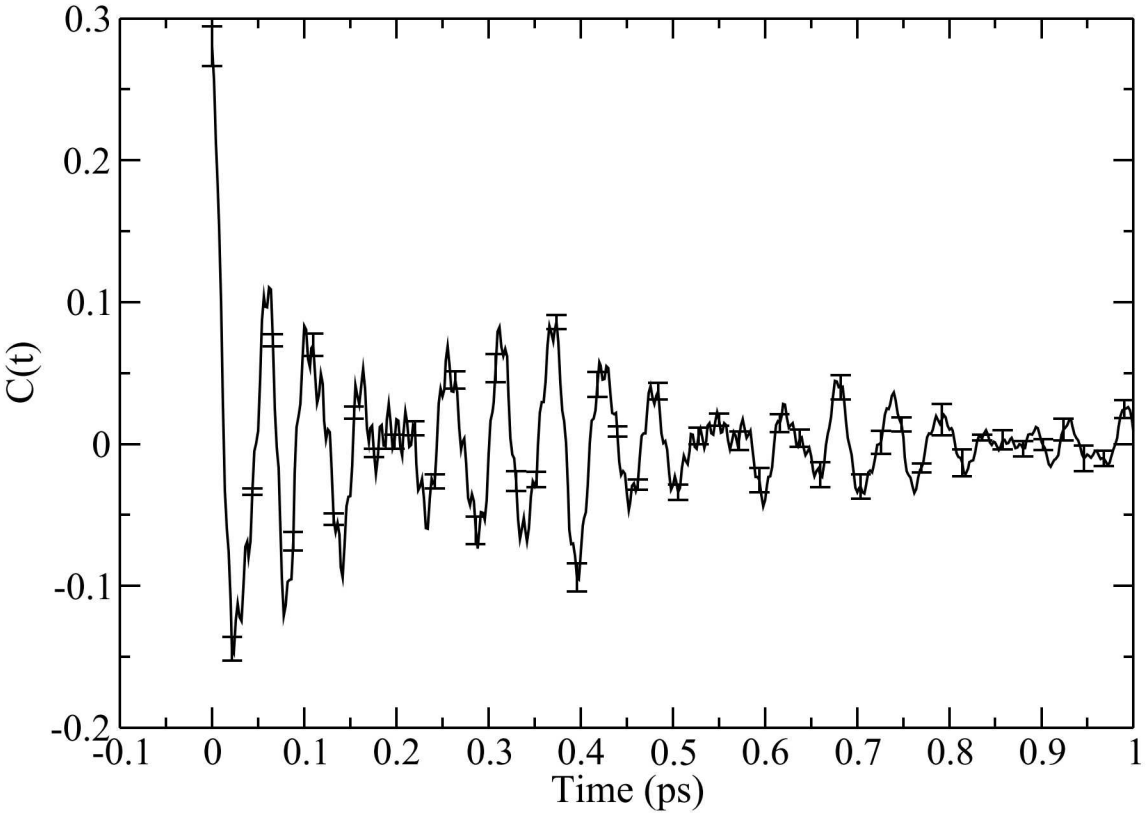

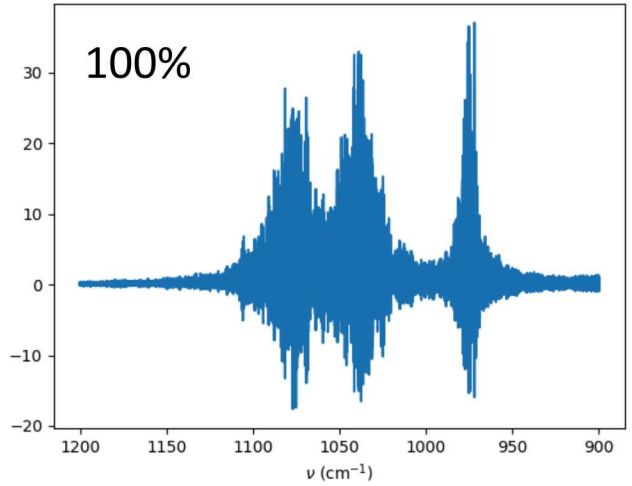

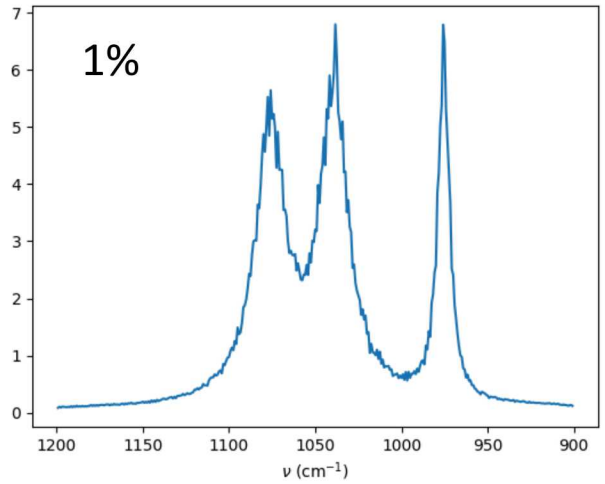

- Error bars calculated with block averaging and the student-T distribution for the 95% confidence interval

from Correlation Functions

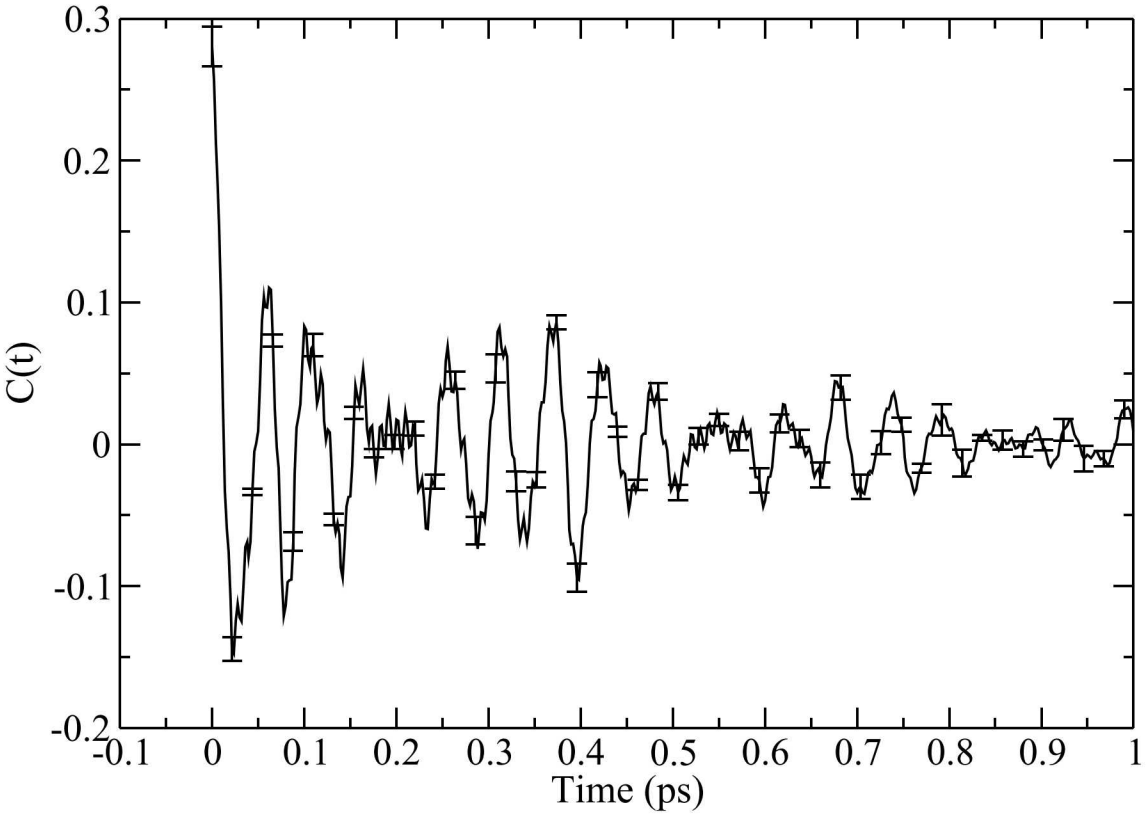

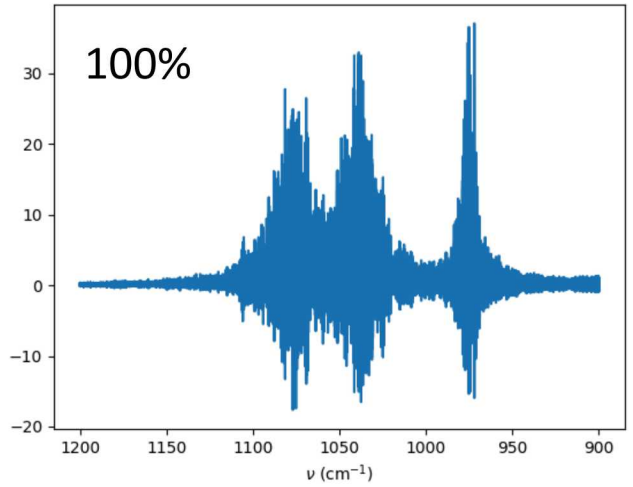

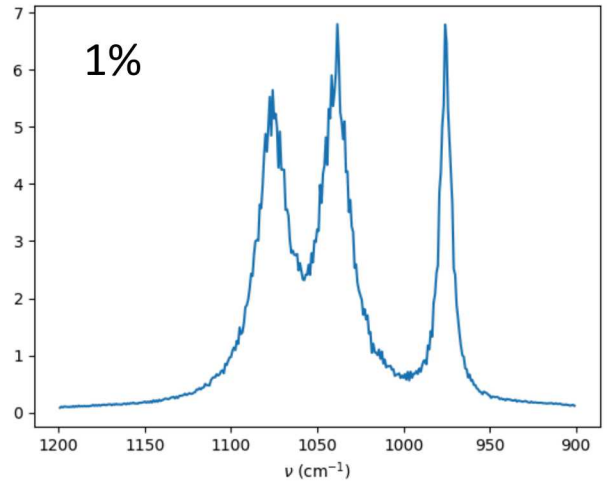

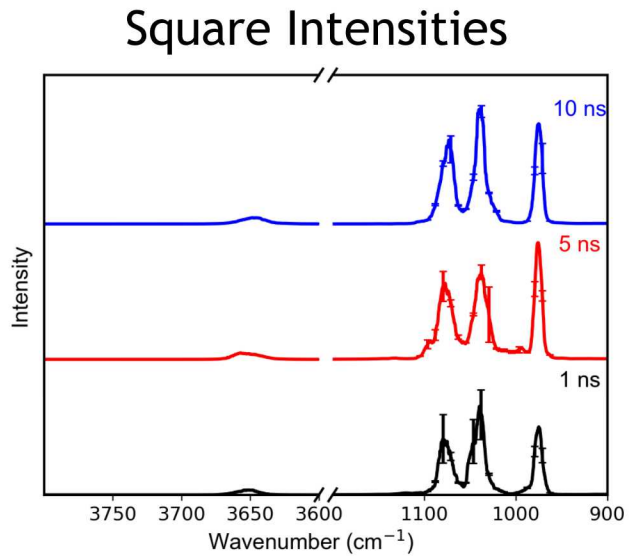

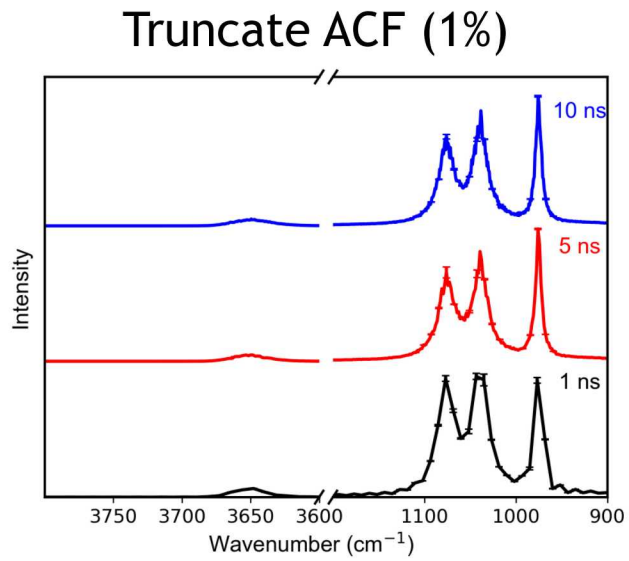

- Error bars calculated with block averaging and the student-T distribution for the 95% confidence interval

# of Angle Bending Term

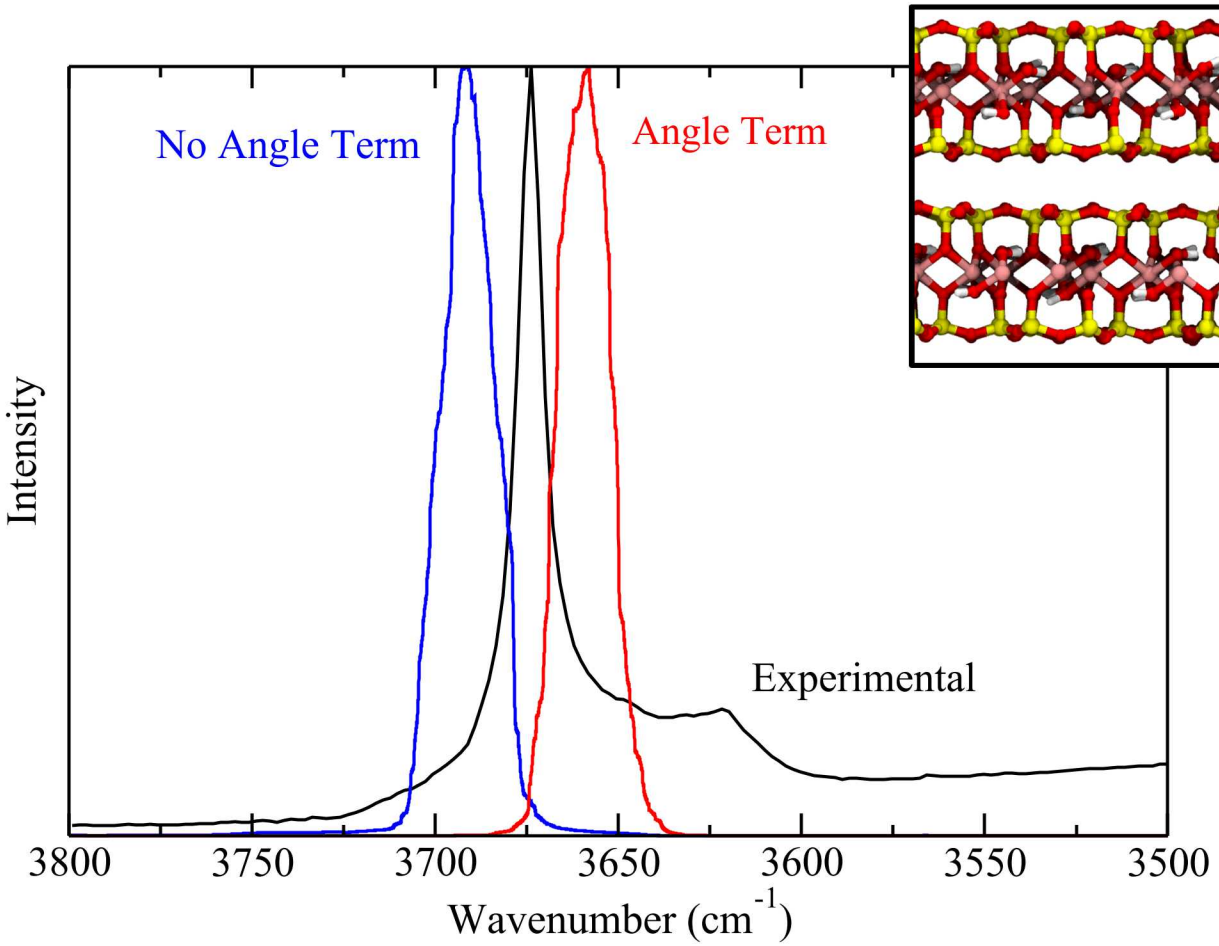

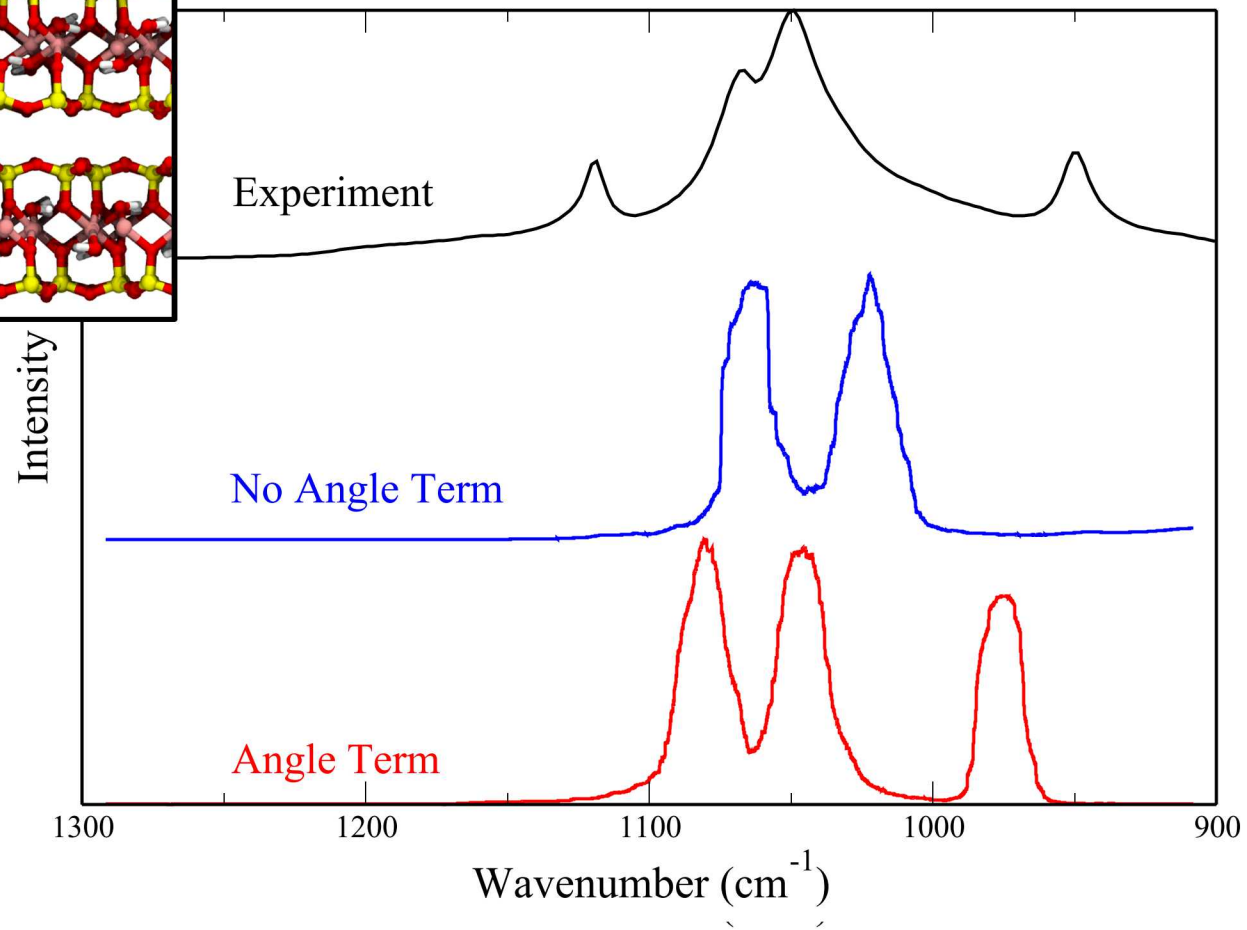

IR Spectrum of (110) Pyrophyllite Edge

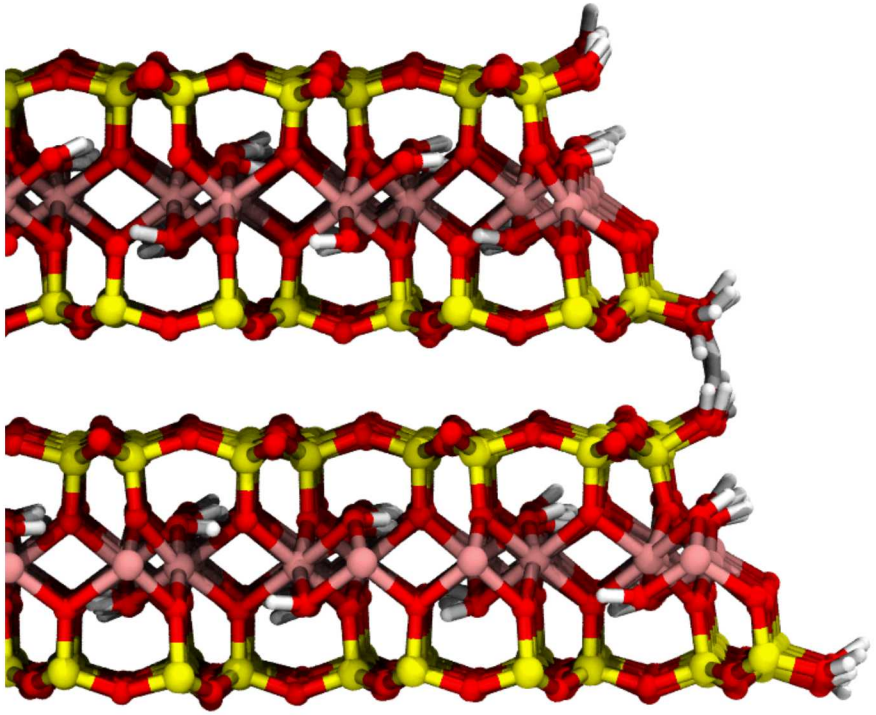

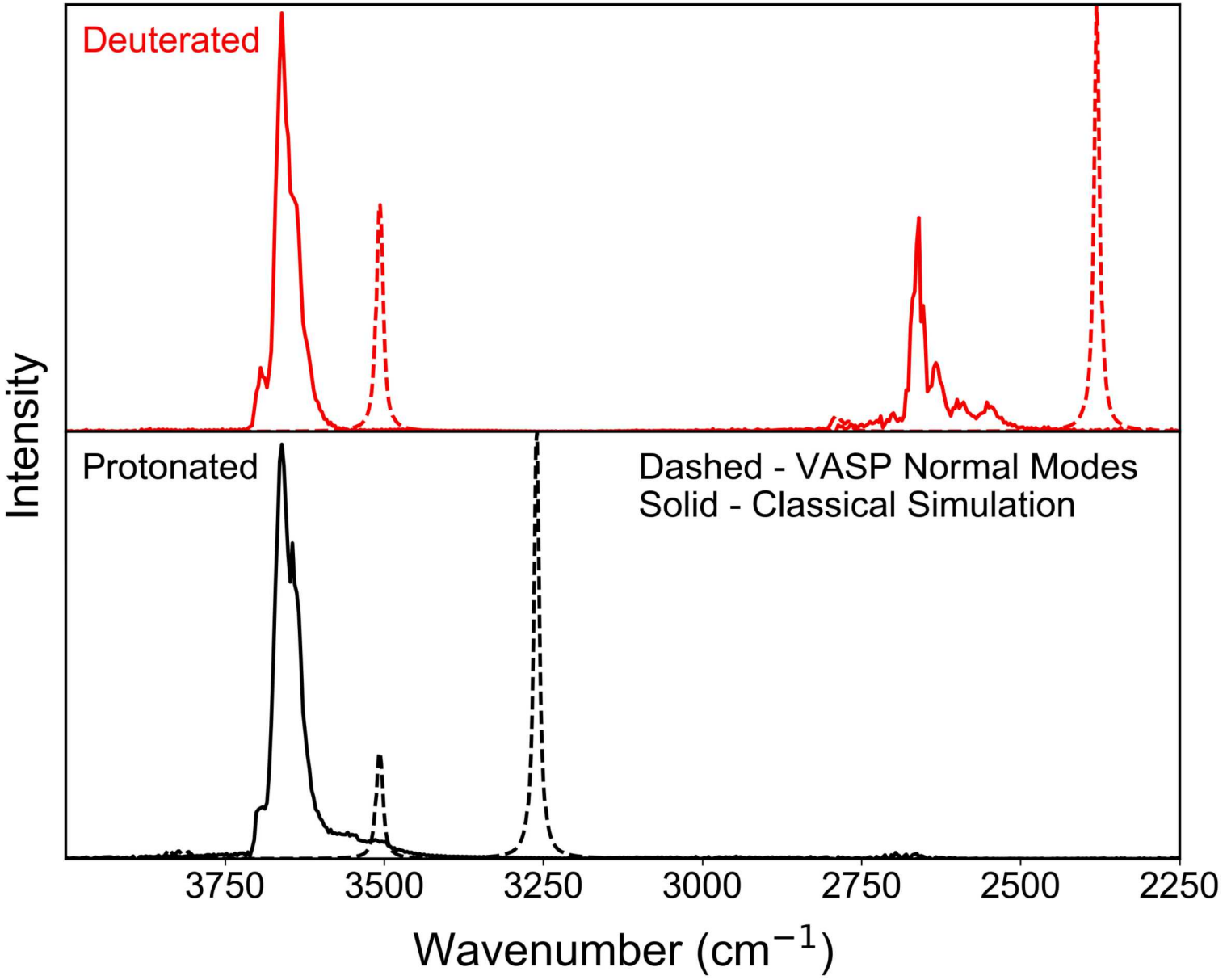

Direct Comparison of Simulated Pyrophyllite Spectrum to Experiments

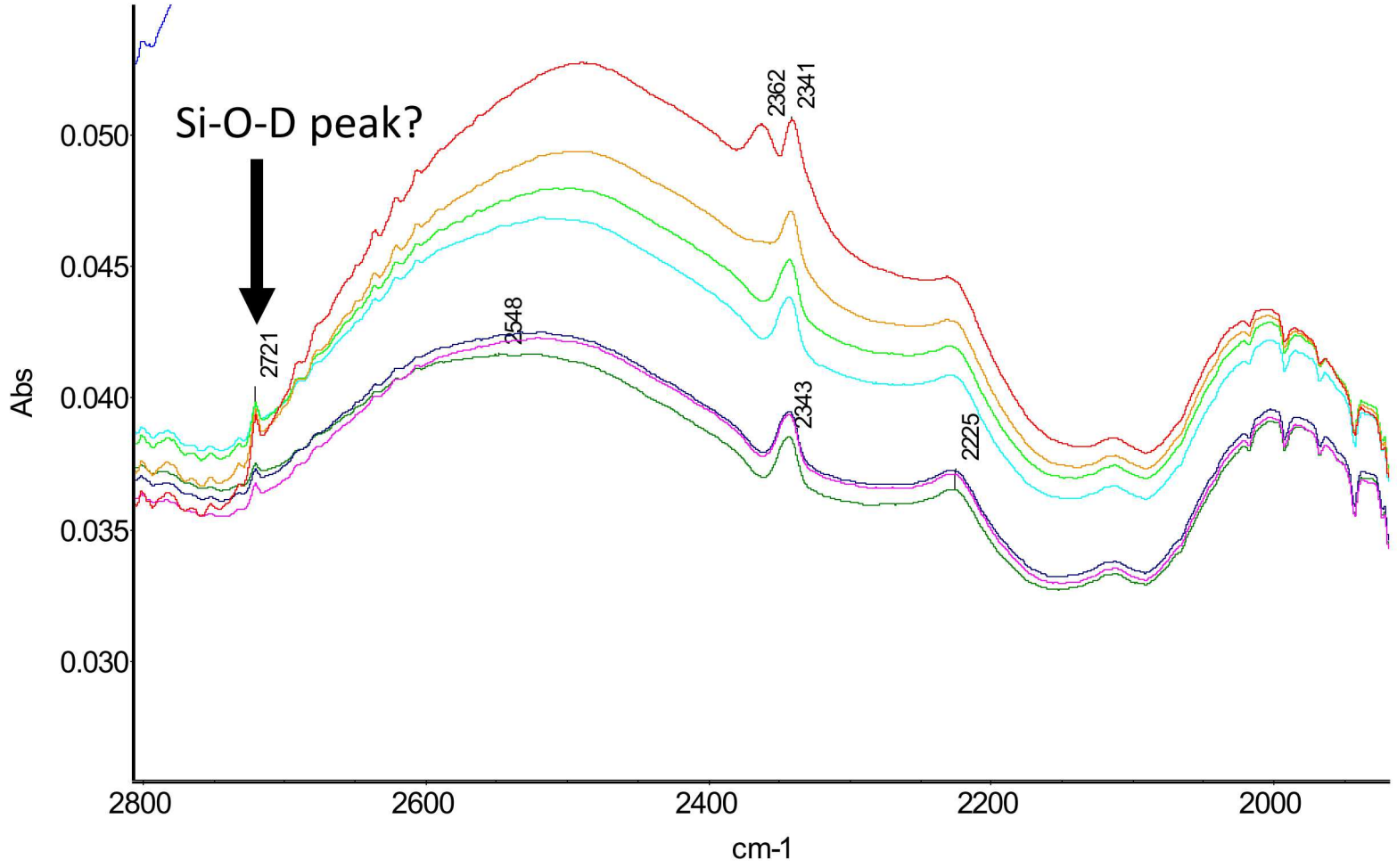

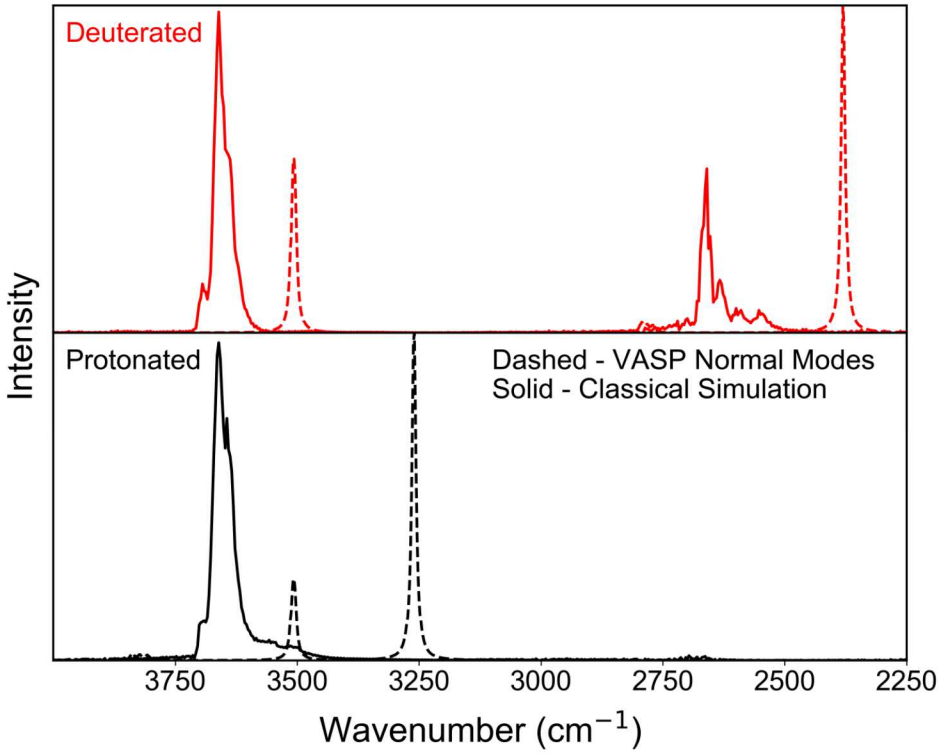

Conclusions

ClayFF angle bending terms improve simulated clay edge structure

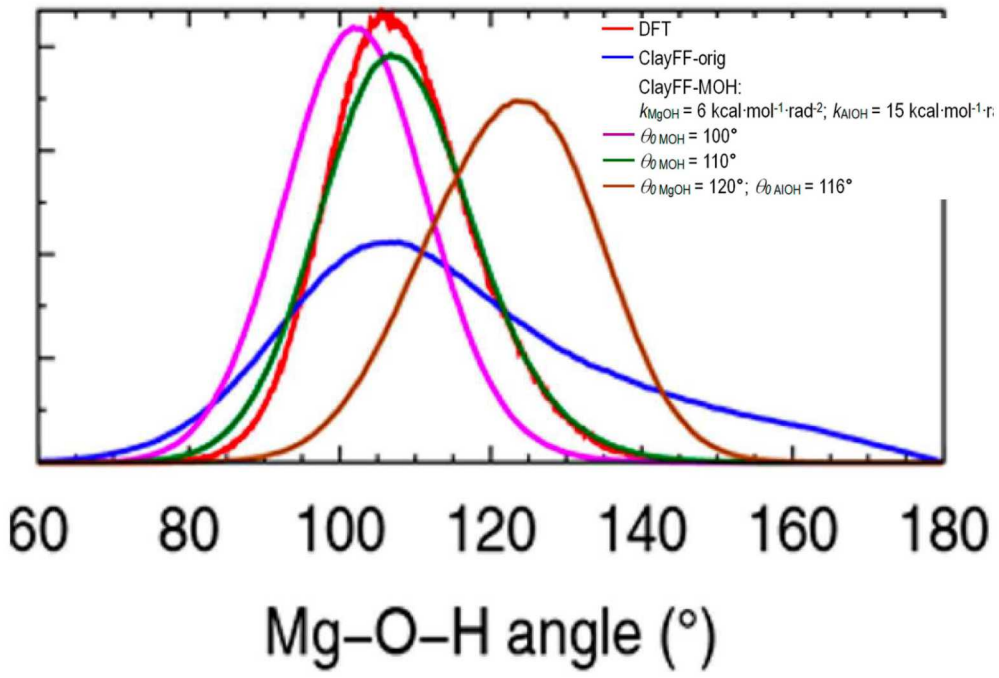

Improved clay structure leads to improved agreement in clay IR spectrum

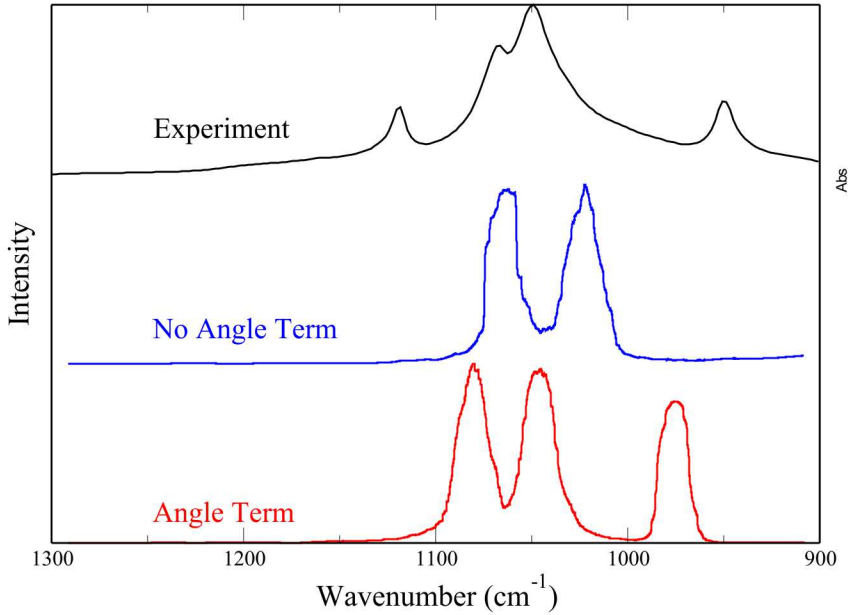

Direct observation of clay edge via IR spectroscopy